JOURNAL OF MATERIALS SCIENCE 19 (1984) 73–81

Adhesion of ice to a flexible substrate

E. H. ANDREWS, H. A. MAJID, N. A. LOCKINGTON
Department of Materials, Queen Mary College, Mile End Road, London E1 4NS, UK

The adhesion of ice to a flexible substrate, polyurethane elastomer, has been studied using the Andrews–Stevenson test procedure which involves the pressurization to failure of an enclosed interfacial crack. The temperature, rate of pressurization and substrate layer thickness were varied and the failure energy (critical energy release rate) determined. If energy release from the flexible substrate is ignored an apparent failure energy is obtained which first increases and then decreases as the layer thickness rises from zero to 4 mm. This thickness effect results in a large variation in the pressure needed to produce failure, and is thus important in relation to the ice-release properties of the substrate. It is shown that the thickness effect can be explained quantitatively in terms of the energy release from the flexible substrate, which, in turn, depends on its visco-elastic properties. The true failure energy is derived and is also found to correlate with the visco-elastic response of the rubber. Finally, these ideas are used to explain the effects of rate and temperature on the conditions of failure.

1. Introduction

The cohesive and adhesive strengths of ice have been widely studied [1]. The cohesive properties, in particular, are found to depend strongly on the technique employed and the testing conditions [2–6]. Measurements at different testing rates are necessary beacuse of the propensity of ice to creep under load [5].

In adhesive measurements it has been established that a transition from a cohesive failure mode (fracture through the ice), to an adhesive mode (failure at the interface), is commonly encountered as the temperature rises towards the melting point [7]. In the adhesive mode, the failure strength is highly rate and temperature dependent [1].

The fracture mechanics approach employed here, and in our previous paper [1], has not been widely used in the study of ice. However, Goodman and Tabor [8] and Goodman [9] measured cohesive fracture energy using the three-point bending of sharply notched beams and a diamond indentation test, while Liu and Miller [10] carried out tests at different rates on "compact tension" specimens. These workers obtained cohesive fracture energy values which generally fell in the range 0.6 to 2.3 $J m^{-2}$. For very slow rates of testing and low temperatures, values as high as 38 $J m^{-2}$ were found, reflecting perhaps, energy dissipated by creep processes.

The adhesion of ice to structures poses a continuing problem to those involved with machines and installations which function in cold outdoor environments. Examples of such structures are aircraft, harbour installations, shipping, radar aerials and overhead cables. It is sometimes possible to take advantage of the intrinsically low surface energy of polymeric materials to reduce the adhesion of ice, and fluorinated polymers appear to be the best in this regard. However, ice adhesion is not a simple phenomenon and consideration has to be given to the conditions of ice formation, the ambient temperature, and the adhesive–cohesive transition temperature, as well as to other factors, before the behaviour of any particular system can be predicted [1].

Apart from the use of low energy surfaces and temporary de-icing fluids, both thermal and mechanical means have been used to ameliorate the problem. But these require ancilliary equipment and are therefore costly and sometimes impracticable. A final idea is that a flexible substrate

0022–2461/84 $03.00 + .12

may shed ice more effectively than a rigid one because of its ability to deflect under load, and it is this suggestion that led to the research reported here.

The system investigated consists of a polyurethane rubber layer bonded to a rigid base, the flexible layer thus acting as a coating. The technique used to remove the ice, once formed, from the substrate is the test introduced by Andrews and Stevenson [11] in which an enclosed circular crack is created at the ice/substrate interface and pressurized internally to failure. This arrangement leads either to interfacial failure or cohesive failure through the ice, according to the relative strengths of interface and bulk ice, and thus lends itself to the investigation of the adhesive–cohesive failure mode transition [1]. Whatever the mode of failure, the failure energy, or critical energy release rate, may be determined using a fracture mechanics analysis [11, 12], thus quantifying the effects observed.

Although the test employed bears a resemblance to the "blister test" described by Dannenberg, Williams and others [13, 14], it is really quite different in that it employs a *thick* specimen. In the blister test the crack radius has to be very much larger than the sheet thickness, whereas a ratio of 1:1 is commonly employed in the Andrews–Stevenson test. This requires a different elastic analysis of which the "blister test" becomes a special case [11].

The work reported here demonstrates that the flexibility of the surface coating does indeed affect the force required to separate the ice from the substrate, but that the dependence is complex and related to the visco-elastic properties of the flexible material as well as to its surface characteristics.

2. Materials

The polyurethane elastomer used was a commercial polyester-based, thermoplastic material, being a reaction product of 4,4 di-phenyl methane di-isocyanate, 1,4 butane diol and a polyester formed from the reaction of adipic acid and a mixture of 1,4 butane diol and 1,6 hexane diol. The material was pigmented and supplied by Elastogran UK Ltd, a BASF company, under the name "Elastollan C80A-10". The material was further characterized by dynamic mechanical spectroscopy (DMS) using a "Rheometrics" dynamic mechanical spectrometer at 1 Hz. A typical trace is shown in Fig. 1 which gives dynamic storage modulus G', loss modulus G'' and $\tan\delta$ as functions of temperature. All materials have a $\tan\delta$ peak in the temperature range -25 to -30°C, and this will be taken as the glass transition temperature range of the substrates.

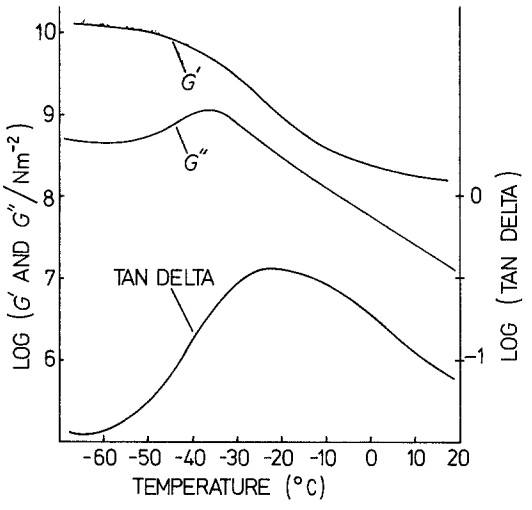

Figure 1 Storage modulus, loss modulus and $\tan\delta$ for polyurethane as functions of temperature.

The ice was cast from distilled water at various temperatures, and was relatively bubble-free on account of the slow freezing caused by the insulating nature of the polyurethane. The effect of bubble content has been reported previously [1].

3. Experimental details

3.1. Specimen preparation

The polyurethane sheet material, of thickness ranging from 0.25 to 3 mm, was bonded to a cylindrical brass base block using a thin film of "Evostik" impact adhesive. The base block contained a central access port and a corresponding hole was cut in the polyurethane. A disc of PTFE, of radius 6.5 mm and thickness 0.27 mm, was placed over the hole before the ice was cast. Casting was accomplished by building a temporary mould around the base block using adhesive tape. The final testpiece configuration is shown in Fig. 2. After casting, the top surface of the ice was levelled using a sharp razor blade as a scraper.

Different sheet thicknesses were obtained in various ways. To begin with, the polyurethane was supplied in a range of thicknesses. Thicknesses below 0.25 mm, however, had to be obtained by hand grinding the mounted sheets on emery paper. In such specimens the unground surface was

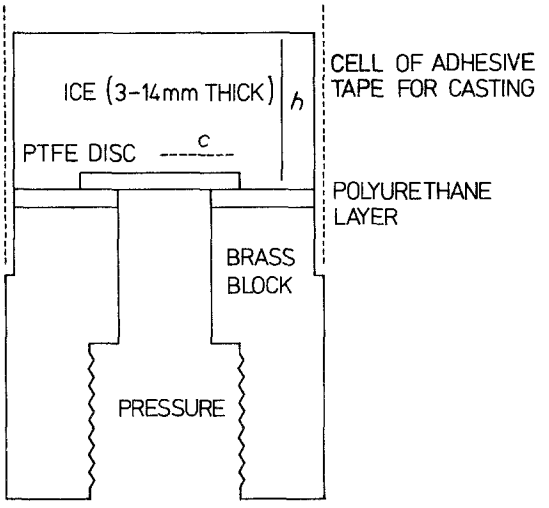

Figure 2 Test specimen configuration for ice/polyurethane adhesion.

presented to the ice. Thicker sheets were also built up by bonding several layers of polyurethane together using "Evostik" impact adhesive.

Before casting the ice, the polyurethane surfaces were cleaned with warm water and detergent, rinsed with distilled water, wiped with acetone and dried.

3.2. Failure energy measurements

The test apparatus and methods have been described fully in previous publications [1, 11] and will not be elaborated here. The test is a simple procedure in which pressure is applied to the internal circular flaw created by non-adherence of the polytetrafluorothylene (PTFE) disc. Pressure is applied through a small bubble of air compressed by hydraulic oil by means of a pump/accumulator system. The pressurization rate can be controlled within certain limits and both this rate and the peak pressure are monitored by means of a pressure transducer and an ultraviolet high speed chart recorder. The failure energy is given by the following formulae:

(a) If the failure is cohesive through the ice

$$2\mathscr{T} = P_c^2 c / E f_1(h/c) \tag{1}$$

$$f_1 = \frac{1}{1-\nu^2}\left\{\frac{3}{32}\left[\left(\frac{c}{h}\right)^3 + \left(\frac{c}{h}\right)\frac{4}{1-\nu}\right] + \frac{1}{\pi}\right\}^{-1} \tag{2}$$

(b) If the failure is adhesive, i.e. interfacial

$$\theta = P_c^2 c / E f_2(h/c) \tag{3}$$

$$f_2 = \frac{1}{1-\nu^2}\left\{\frac{3}{32}\left[\left(\frac{c}{h}\right)^3 + \left(\frac{c}{h}\right)\frac{4}{1-\nu}\right] + \frac{2}{\pi}\right\}^{-1} \tag{4}$$

where P_c is the critical pressure for failure, c is the radius of the artificial flaw, E is the Young's modulus of ice (taken as 8.5 GN m^{-2}), h is the height of ice above the flaw, and ν is the Poisson's ratio for ice (taken as 0.35) [1].

These formulae assume that the substrate is rigid and that energy release therefore derives only from the strain field in the ice. The quantities calculated on this basis will therefore be called $2\mathscr{T}$(app) and θ(app), being only the apparent values of the critical energy release rate. The corresponding true (i.e. total) parameters will be denoted $2\mathscr{T}$ and θ in the normal manner. The modulus E of ice varies by only 2% between -5, and $-20°$C and will be assumed to be independent of temperature [1].

4. Theory of thickness dependence

In order to obtain the true critical energy release rates at failure we must consider the energy release from the flexible substrate layer. This may be calculated as follows.

In what follows, parameters relating to the rubberlike layer will be indicated by a prime. Thus h is the thickness of the ice and h' that of the polyurethane.

Consider a plan view of the specimen (Fig. 3).

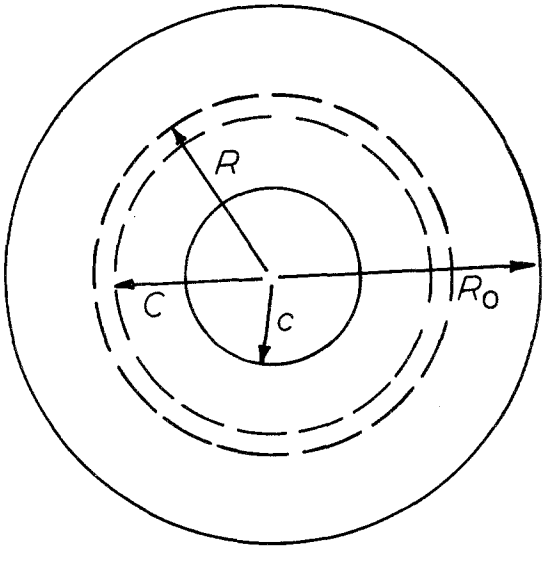

Figure 3 Schematic plan view of propagating crack (used in calculating the energy release rate).

Let C be the instantaneous radius of the crack and R the radius at and above which the stored energy density in the flexible layer becomes independent of radius. Thus the region $C<r<R$ is the region of stress concentration ahead of the crack. Let $R=\lambda C$.

If the crack grows by an amount ΔC, the new crack area created is

$$\Delta A = 2\pi C\Delta C. \tag{5}$$

The energy lost from the "constant energy" region at $r>R$ consequent upon this crack advance is

$$-\Delta\mathscr{E}' = 2\pi R\Delta R W_0' h' \tag{6}$$

where W_0' is the energy density in the "constant energy" region and h' the thickness of the flexible layer. Then,

$$-\frac{\Delta\mathscr{E}'}{\Delta A} = \lambda^2 W_0' h'. \tag{7}$$

The energy density in the flexible layer is assumed to be given by the linear formula

$$W_0' = \sigma^2/2E' \tag{8}$$

where σ is the stress normal to the plane of the layer and E' is the effective modulus. Because of the thinness of the rubber layer the strains are likely to be small away from the crack tip and the outer perimeter, and this justifies the linear formula for W_0'. We shall see later, however, that the assumption of linearity breaks down at temperatures close to 0° C where shear slippage at the ice–rubber interface relieves the constraints upon the rubber.

The stress σ is given approximately by averaging the resistance to the pressure in the crack, over the adhering area. This assumes of course that the high stresses near the crack and the lower stresses at the outer perimeter (due to the more compliant configuration near a free edge) represent only a small net perturbation of the average stress. Then,

$$\sigma = \frac{C^2 p}{(R_0^2 - C^2)} \tag{9}$$

where R_0 is the outer radius of the specimen.

We thus obtain, from Equations 8 and 9, the energy release rate from the flexible layer as,

$$-\frac{\Delta\mathscr{E}'}{\Delta A} = \frac{\lambda^2 h' C^4 P^2}{2E'(R_0^2 - C^2)^2} \tag{10}$$

$$= \frac{h'P^2}{2E'}\left[\frac{\lambda}{(R_0/C)^2 - 1}\right]^2. \tag{11}$$

Let

$$\frac{1}{2}\left[\frac{\lambda}{(R_0/C)^2 - 1}\right]^2 \equiv \mu. \tag{12}$$

The total energy release rate is then

$$-\frac{\Delta\mathscr{E}}{\Delta A} = \frac{P^2 C}{Ef(h/c)} + \frac{P^2 h'\mu}{E'} \tag{13}$$

$$= \frac{P^2 C}{Ef(h/c)}\left[1 + \frac{h'}{c} f(h/c)\mu\frac{E}{E'}\right] \tag{14}$$

where $f(h/c)$ is either $f_1(h/c)$ or $f_2(h/c)$ depending on the mode of failure. Thus at the critical pressure the true failure energies are

$$2\mathscr{T} = 2\mathscr{T}(\text{app})(1 + af_1(h/c)h') \tag{15}$$

$$\theta = \theta(\text{app})(1 + af_2(h/c)h') \tag{16}$$

where

$$a = \mu E/cE'. \tag{17}$$

A plot of $1/(2\mathscr{T})(\text{app})$ against $f_1(h/c)h'$ or of $1/\theta(\text{app})$ against $f_2(h/c)h'$ should therefore give a straight line with an intercept at $h'=0$ of $1/(2\mathscr{T})$ or $1/\theta$ and a slope, s, of $a/(2\mathscr{T})$ or a/θ.

The effective modulus of the rubberlike layer is then given by

$$E' = \frac{\mu E}{ca} = \frac{\mu E}{c}\frac{1}{2\mathscr{T}s} \tag{18}$$

or the equivalent equation for adhesive failure.

To estimate a value for μ we may assume that $\lambda \sim 1.2$ and $C=c$ (i.e. the point of initiation). This gives $\mu \simeq 1/8$. The value of E is taken as 8.5 GN m^{-2} and $c=6.5$ mm.

5. Results

5.1. Thickness dependence

Typical results for thickness dependence are shown in Fig. 4 where $2\mathscr{T}(\text{app})$ or $\theta(\text{app})$ is plotted against the thickness of the polyurethane sheet. Although these failure energies are apparent quantities, it must be stressed that they are directly related to the pressure required to produce failure and thus to the ease or difficulty of ice removal. The variation of the apparent failure energy with thickness is therefore an effect with great practical significance.

There is something like a tenfold decrease in the apparent failure energy as the thickness of the polyurethane varies from 0.1 to 3.0 mm and this corresponds to a threefold variation in critical pressure. Clearly, the energy release from the flexible substrate assists ice removal at a given pressure in proportion to the substrate thickness. At poly-

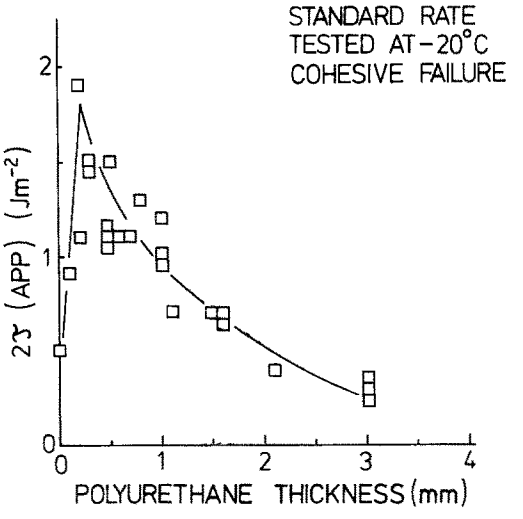

Figure 4 Effect of rubber-layer thickness on the apparent failure energy.

urethane thickness approaching zero, there is evidence of a reversal of this effect. The data at effectively zero thickness was obtained from brass specimens painted with a thin layer of polyurethane paint and give a lower failure energy than the thinnest sheet polyurethane (some 0.1 mm thick). Such a reversal is to be expected, since the true failure energy $2\mathscr{T}$ or θ obtained by extrapolating the data to zero thickness, assumes that the energy absorbed in crack propagation is independent of thickness. This cannot be the case when thickness approaches zero, since most of the energy absorption occurs through visco-elastic losses in the rubber. When the volume of rubber approaches zero, a fall in $2\mathscr{T}$ or θ is therefore bound to result. The sheet thickness at which this reversal takes place will be determined by the linear size of the highly stressed region around the crack tip, and our results show that this is approximately 0.1 mm.

The data of Fig. 4 has been replotted in Fig. 5 in the form indicated by our theoretical Equations 15 and 16, that is, as a graph of $1/2\mathscr{T}$ or $1/\theta$ against $f(h/c)h'$. Neglecting the "zero thickness" point, the theoretical prediction is borne out, there being a linear dependence and intercept as expected. All results from this point onwards will be presented in terms of the two parameters which define the relationship in Fig. 5, namely the intercept or its reciprocal $2\mathscr{T}$ or θ, and the slopes of the line.

Where possible, the slopes and intercepts have been determined by least squares. In some cases, however, there is a disproportionate influence of points at small $2\mathscr{T}$ where accuracy of measurement is poor. This results in large standard errors and even in negative intercept values. In such cases a visual judgement of the best straight line through the points is more satisfactory. At temperatures approaching the melting point of ice (above $-2°$ C) some definite nonlinearity appears in these plots and will be discussed later.

The collected data for slopes and intercepts are shown in Figs. 6 and 7 for the two pressurization rates employed (see below). There is a consistent trend according to which the intercept increases, and the slope decreases, as the temperature falls. These diagrams also indicate the mode of failure observed, namely cohesive, adhesive or mixed. In harmony with earlier findings using metal substrates [1], there is a transition from cohesive

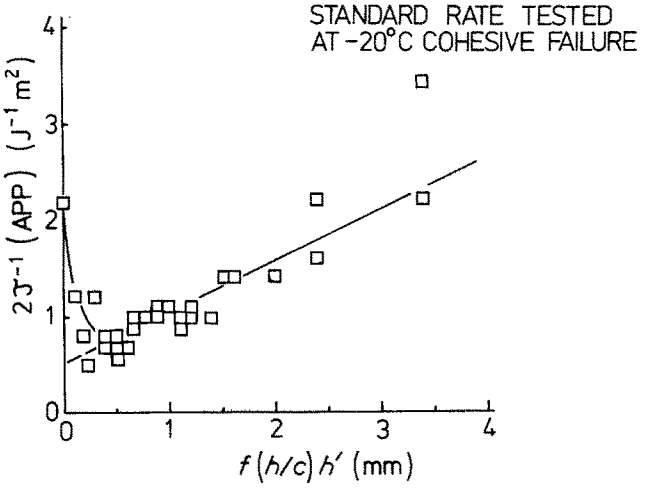

Figure 5 Reciprocal failure energy plotted against normalized thickness parameter.

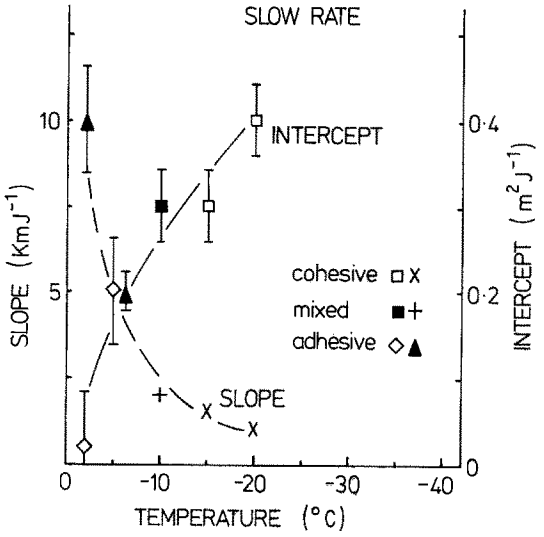

Figure 6 Slopes and intercepts from plots of the kind shown in Fig. 5, as functions of test temperature at slow pressurization rate.

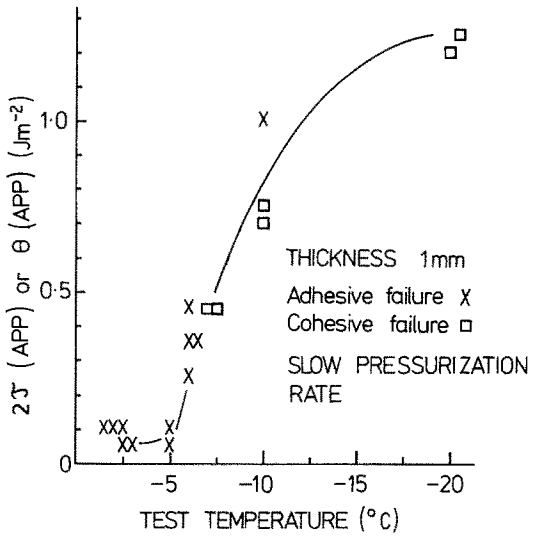

Figure 8 Effect of temperature on apparent failure energies at slow pressurization rate.

to adhesive failure as the temperature rises towards the melting point of the ice. This transition temperature is around -10° C for slow pressurization and -5° C for fast. It is also of note that in mixed-mode cases, failure is cohesive at small thicknesses (high $2\mathscr{T}$), and adhesive at large thicknesses, of the rubber layer. The transition tends to occur at around $2\mathscr{T} = 1\ \mathrm{J\,m^{-2}}$.

5.2. Rate and temperature dependence

Fig. 8 shows the temperature dependence of the apparent failure energy at slow pressurization rates

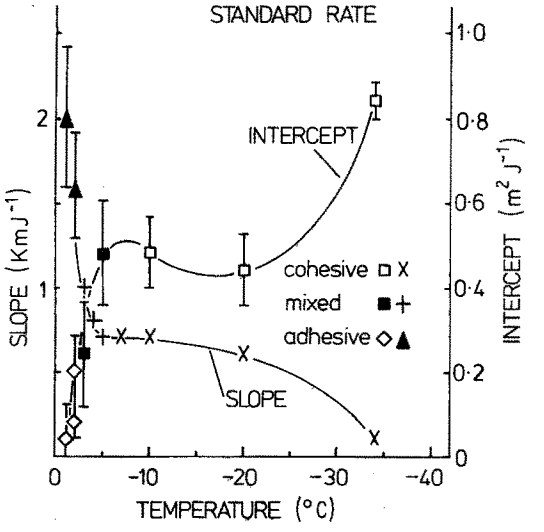

Figure 7 As Fig. 6 but at standard pressurization rate.

(failure in 0.4 to 0.9 sec) for a polyurethane layer 1.0 mm thick. The variable in this plot is the testing temperature; the ice making temperature was -20° C in all cases. A strong temperature effect is apparent, the failure energy rising sharply with falling temperature.

At "standard" pressurization rate (failure in 0.07 to 0.10 sec), the behaviour is quite different, as indicated in Fig. 9. Now the data are relatively insensitive to temperature except in the region just below 0° C. It is clear that there is some time–temperature interdependence and this is reminiscent of the effect of rate upon the cohesive–adhesive transition temperature observed previously [1]. In the present case this effect may be amplified by the visco-elasticity of the rubber layer.

The situation becomes somewhat clearer when we consider the temperature dependence of the two parameters referred to earlier. Fig. 10 shows the variation of $2\mathscr{T}$ or θ (the reciprocal intercept of such plots as Fig. 5) with testing temperature for both slow and standard pressurization rates. This true failure energy should be the actual energy required to drive the crack against energy losses in the rubber and the ice. The energy falls more than tenfold over the range to -34° C, with a plateau in the curve between -10 and -20° C.

Much of the failure energy should result from visco-elastic energy losses in the rubber, and to test this idea we have plotted on the same axes in Fig. 10 the loss factor, $\tan\delta$ of the polyurethane

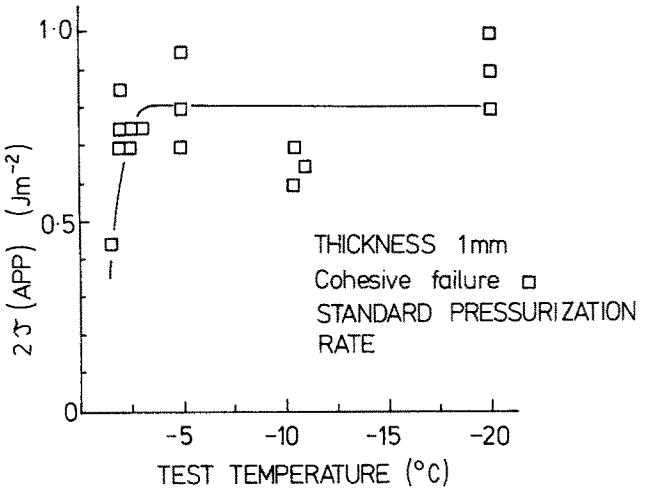

Figure 9 As Fig. 8 but for standard pressurization rate.

at 1 Hz. The vertical scale was adjusted to fit at low temperature. The loss tangent does indeed follow the failure energy curve well at temperatures below about -15°C, but not above this point where the failure energy rises steeply. It could be argued that the frequency of 1 Hz is too low, considering the velocity of the propagating crack. The loss peak in polyurethane, typically, rises by 4°C for every decade increase in rate. However, the failure energy measured refers to crack *initiation*, at which condition the crack is accelerating from its initial zero velocity. This fact, together with the breadth of the loss peak, suggests that no great error is introduced by fitting the 1 Hz loss curve.

The data of Fig. 10 may be explained qualitatively as follows. Below about -10 to -15°C, the interfacial bond between ice and rubber is strong and failure is cohesive in the ice. No shear slippage can occur at the interface and the rubber is thus highly constrained and the deformations small. In this region, $\tan\delta$ reflects accurately the energy losses in the rubber and therefore correlates well with $2\mathcal{T}$. Above about -10°C, the transition to adhesive failure begins to occur, and interfacial shear is possible on account of a "liquid-like" layer at the ice surface (see discussion in [1]). As a consequence of interfacial slippage, the constraints upon the rubber are greatly relaxed and deformations become larger. Energy losses in visco-elastic materials are known to increase greatly with strain [15] and the failure energy increases accordingly. Clearly, at 0°C the failure energy must collapse to zero, but even at -2°C the effect of large strain still dominates. This 'high temperature' loss mechanism comes into operation at and above the cohesive–adhesive transition temperature. Since the transition temperature is highly rate-dependent even in the *absence* of a visco-elastic substrate (see [1]), this accounts for the dramatic effect of a small rate change demonstrated in Figs. 8 and 9.

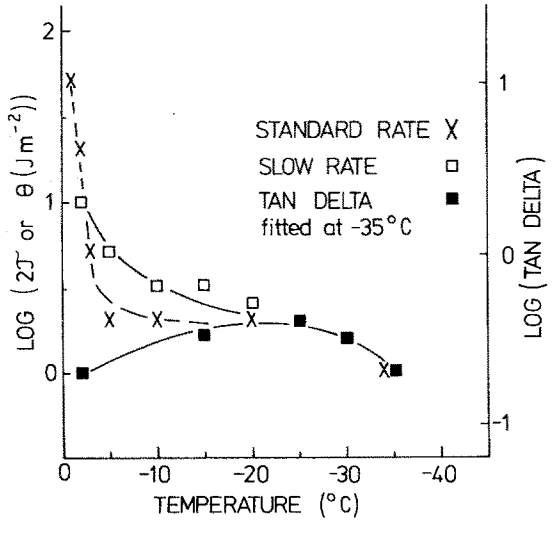

Figure 10 Comparison of failure energies with $\tan\delta$ for the polyurethane ($\tan\delta$ data fitted at -35°C).

Fig. 11 is obtained from the temperature dependence of the second parameter, the slopes of such plots as Fig. 5. When multiplied by $2\mathcal{T}$ or θ, this parameter is inversely proportional to the effective modulus E' of the rubber, assuming a constant value for the Young's modulus of ice [1]. The absolute values predicted for E' are obtained from Equation 18 and plotted as a function of temperature for both pressurization rates employed. In Fig. 11 also is included a plot of the dynamic shear modulus G' for the polyurethane from DMS.

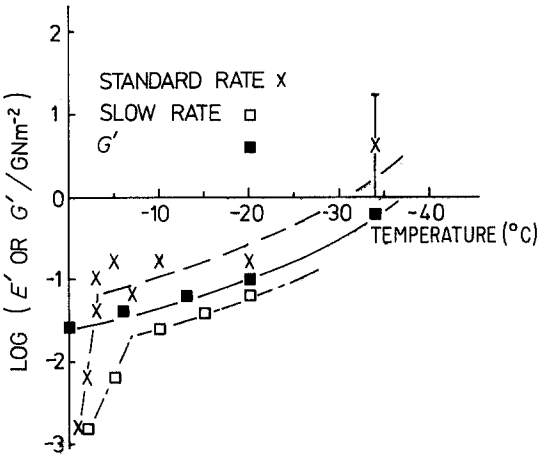

Figure 11 Comparison of predicted modulus E' with storage modulus G' for the polyurethane (absolute values, no fitting).

The agreement between E' and G' is good at temperatures below $-5°$ C, both as regards temperature dependence and absolute values. The predicted E' for slow pressurization is only 25% of that for the higher rate, demonstrating the correct relationship for a visco-elastic rate dependence. The G' curve for 1 Hz lies between the E' curves and within a factor of about two of either of them. It should be remembered of course that for elastic solids, $G = E/2(1 + \nu)$ where ν is Poisson's ratio.

Above about $-5°$C the E' curves depart strongly from G', falling rapidly to very low values. This fall in E' can be compared with the rise in θ observed over just the same temperature range and attributed to the onset of shear slippage at the interface leading to larger deformations in the rubber.

This explanation fits neatly with the E' data, since E', the effective modulus, must reflect the increased compliance caused by interfacial slip. The sudden drop in E' occurs at $-7°$C for slow pressurization and $-3°$C for the faster rate, and this is again in harmony with the adhesive/cohesive transition range observed in Figs. 6 and 7 and with the behaviour of θ displayed in Fig. 10.

One difficulty with the above explanation is that the absolute value of E' for temperatures above the transition is much lower than G', which at first sight seems impossible. However, it must be remembered that G' measurements are made at very small strains and that elastomers, especially when they contain fillers, have stress–strain curves which are concave to the strain axis at moderate strains. The effective (tangent) modulus therefore decreases with increasing strain, and stored energy increases faster than the square of the stress. This behaviour is not reflected by our assumptions of linearity, and would produce exactly the effects noted at temperatures close to 0° C where interfacial slippage permits relatively large strains to occur in the polyurethane layer.

5.3. Further observation on the effects of rate

In earlier studies of the adhesive failure of epoxy resin [11], it was shown that the rate of pressurization was not a measure of the true rate of the experiment. Crack velocity was found to be a much more valid rate parameter. It was not possible to measure crack velocity in the present work and we therefore do not have a reliable rate determining variable. Nevertheless, rate effects have been noted above and it seemed worthwhile to see how far the rate of pressurization could be used to characterize these effects. An example of the result is shown in Fig. 12. A normalized form of $2\mathcal{T}$ was used to eliminate the effects of thickness using the kind of data shown in Fig. 5. The value of $2\mathcal{T} = 1$ was left unchanged and all other $2\mathcal{T}$ values multiplied by the appropriate factor to produce a thickness-independent quantity. This normalized $2\mathcal{T}$ was then plotted against the rate of pressurization defined as the time to failure divided by the critical failure pressure. Both these quantities, of course, can be found from the chart recorder trace.

The data shown in Fig. 12 relate to a test temperature of $-20°$ C and exhibit the expected scatter. There is, however, a definite indication of a peak which is again suggestive of visco-elastic loss processes. The peak does not appear in data collected at higher temperatures. It is clearly desirable to develop methods of measuring crack velocity in order to define the experimental rate more precisely.

6. Conclusions

The complex dependence of the apparent failure energy (whether adhesive or cohesive) between ice and polyurethane, upon polyurethane layer thickness, temperature and rate, has been traced to two effects. The first of these is the storage of energy in the rubber layer which is then available to drive the crack. This means that the thicker rubber layers give rise to lower apparent failure

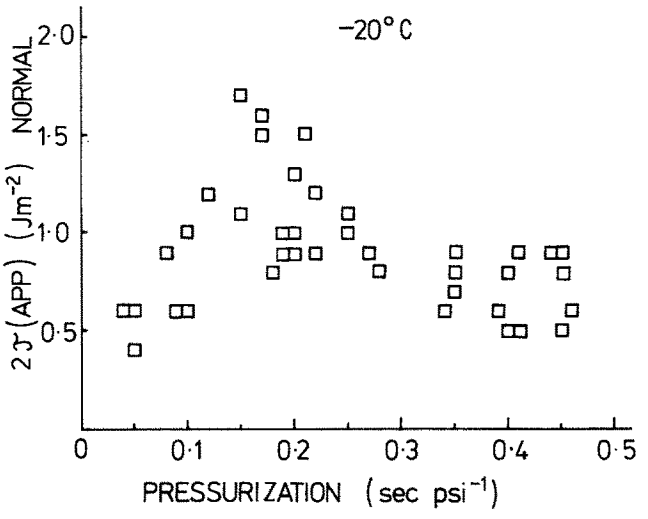

Figure 12 Failure energy at −20° C plotted against pressurization rate showing an apparent peak.

energies and thus to ice release at lower pressures. The effect of layer thickness is given quantitatively by a fairly simple theory based upon this idea of energy storage.

The second effect is the variation of the viscoelastic properties of the polyurethane with temperature and rate. This affects the results in two ways. Firstly, the variation of storage modulus affects the energy stored in the layer and thus its contribution to energy release as the crack propagates. Secondly, the variation of the loss modulus affects the energy dissipated in the rubber around the propagating crack and thus controls the true failure energy. Once again, theory gives quite reasonable agreement with experiment. A corollary of this is that the true failure energy decreases with layer thickness when the latter becomes comparable with the size of the highly stressed region around the crack tip. Our results show that this critical thickness is around 0.1 mm.

Acknowledgements

Thanks are due to the Procurement Executive, Ministry of Defence, for the financial support of this research, and to Dr H. Spell of the Dow Chemical Company for providing DMS data.

References

1. E. H. ANDREWS and N. A. LOCKINGTON, *J. Mater Sci.* **18** (1983) 1455.
2. P. V. HOBBS, "Ice Physics" (Clarendon Press, Oxford, 1974).
3. H. H. G. JELLINEK, *Proc. Phys. Soc. (Lond.)* **71** (1958) 797.
4. I. HAWKES and M. MELLOR, *J. Glaciology* **11** (1972) 103.
5. H. C. WU, K. J. CHANG and J. SCHWARZ, *Eng. Fract. Mech.* 8 (1976) 365.
6. L. W. GOLD, *Canadian J. Phys.* **41** (1963) 1712.
7. H. H. G. JELLINEK, *J. Coll. Interface Sci.* **25** (1967) 192.
8. D. J. GOODMAN and D. TABOR, *J. Glaciology* **21** (1978) 651.
9. D. J. GOODMAN, "Physics and Mechanics of Ice", edited by P. Tryde (Springer Verlag, Berlin, 1980) p. 129.
10. H. W. LIU and K. J. MILLER, *J. Glaciology* **22** (1979) 135.
11. E. H. ANDREWS and A. STEVENSON, *J. Mater. Sci.* **13** (1978) 1680.
12. E. H. ANDREWS, HE PINGSHEN and C. VLACHOS, *Proc. Roy. Soc. (Lond.) A.* **381** (1982) 345.
13. H. DANNENBERG, *J. Appl. Polym. Sci.* **14** (1971) 125.
14. S. BENNETT, K. DE VRIES and M. L. WILLIAMS, *Int. J. Fract.* **10** (1974) 33.
15. E. H. ANDREWS and Y. FUKAHORI, *J. Mater. Sci.* **12** (1977) 1307.

Received 13 January
and accepted 26 April 1983